PCCP

Radiation-Induced Effects on the Extraction Properties of Hexa-n-octylnitrilo-triacetamide (HONTA) Complexes of Americium and Europium

Journal:	*Physical Chemistry Chemical Physics*
Manuscript ID	CP-ART-11-2020-005720.R1
Article Type:	Paper
Date Submitted by the Author:	04-Dec-2020
Complete List of Authors:	Toigawa, Tomohiro; Japan Atomic Energy Agency Peterman, Dean; Idaho National Laboratory, 1765 N. Yellowstone Hwy Meeker, David; Idaho National Laboratory, Center for Radiation Chemistry Research; Florida State University, Department of Chemistry & Biochemistry Grimes, Travis; Idaho National Laboratory, Aqueous Separations and Radiochemistry Zalupski, Peter; Idaho National Laboratory, Aqueous Separations and Radiochemistry Mezyk, Stephen; California State University at Long Beach, Chemistry and Biochemistry Cook, Andrew; Brookhaven National Laboratory, Chemistry Department Yamashita, Shinichi; The University of Tokyo Graduate School of Engineering School of Engineering, Nuclear Professional School kumagai, yuta; Japan Atomic Energy Agency, Nuclear Science and Engineering Center matsumura, tatsuro; Japan Atomic Energy Agency Horne, Gregory; Idaho National Laboratory, Center for Radiation Chemistry Research

ARTICLE

Radiation-Induced Effects on the Extraction Properties of Hexa-*n*-octylnitrilo-triacetamide (HONTA) Complexes of Americium and Europium

Received 30th October 2020,
Accepted 00th December 2020

DOI: 10.1039/x0xx00000x

Tomohiro Toigawa,[a]* Dean R. Peterman,[b] David S. Meeker,[b] Travis S. Grimes,[b] Peter R. Zalupski,[b] Stephen P. Mezyk,[c] Andrew R. Cook,[d] Shinichi Yamashita,[e] Yuta Kumagai,[a] Tatsuro Matsumura,[a] and Gregory P. Horne[b]*

The candidate An(III)/Ln(III) separation ligand hexa-*n*-octylnitrilo-triacetamide (HONTA) was irradiated under envisioned SELECT (Solvent Extraction from Liquid waste using Extractants of CHON-type for Transmutation) process conditions (*n*-dodecane/0.1 M HNO_3) using a solvent test loop in conjunction with cobalt-60 gamma irradiation. The extent of HONTA radiolysis and complimentary degradation product formation was quantified by HPLC-ESI-MS/MS. Further, the impact of HONTA radiolysis on process performance was evaluated by measuring the change in ^{243}Am and ^{154}Eu distribution ratios as a function of absorbed gamma dose. HONTA was found to decay exponentially with increasing dose, affording a dose coefficient of d = (4.48 ± 0.19) × 10^{-3} kGy^{-1}. Multiple degradation products were detected by HPLC-ESI-MS/MS with dioctylamine being the dominant quantifiable species. Both ^{243}Am and ^{154}Eu distribution ratios exhibited an induction period of ~70 kGy for extraction (0.1 M HNO_3) and back-extraction (4.0 M HNO_3) conditions, after which both values decreased with absorbed dose. The decrease in distribution ratios was attributed to a combination of the destruction of HONTA and ingrowth of dioctylamine, which is capable of interfering in metal ion complexation. The loss of HONTA with absorbed gamma dose was predominantly attributed to its reaction with the *n*-dodecane radical cation ($R^{\bullet+}$). These $R^{\bullet+}$ reaction kinetics were measured for HONTA and its ^{243}Am and ^{154}Eu complexes using picosecond pulsed electron radiolysis techniques. All three second-order rate coefficients (k) were essentially diffusion limited in *n*-dodecane indicating a significant reaction pathway: k(HONTA + $R^{\bullet+}$) = (7.6 ± 0.8) × 10^9 M^{-1} s^{-1}, k(Am(HONTA)$_2$ + $R^{\bullet+}$) = (7.1 ± 0.7) × 10^{10} M^{-1} s^{-1}, and k(Eu(HONTA)$_2$ + $R^{\bullet+}$) = (9.5 ± 0.5) × 10^{10} M^{-1} s^{-1}. HONTA-metal ion complexation afforded an order-of-magnitude increase in rate coefficient. Additional nanosecond time-resolved measurements showed that both direct and indirect HONTA radiolysis yielded the short-lived (< 100 ns) HONTA radical cation and a second long-lived (µs) species identified as the HONTA triplet excited state. The latter was confirmed by a series of oxygen quenching picosecond pulsed electron measurements, affording a quenching rate coefficient of k(^{3}[HONTA]* + O_2) = 2.2 × 10^8 M^{-1} s^{-1}. Overall, both the HONTA radical cation and triplet excited state are important precursors to the suite of measured HONTA degradation products.

Introduction

Efficient separation of the trivalent minor actinides (MA) from the trivalent lanthanides (Ln) is one of the major challenges for the development and innovation of advanced used nuclear fuel (UNF) reprocessing technologies. This separation is difficult to achieve due to the chemical similarities of the trivalent *f*-elements,[1-4] and yet critical for the success of proposed Partitioning and Transmutation (P&T) strategies for the conversion of long-lived MA into short-lived radionuclides.[5] Several trivalent MA/Ln separation processes have been developed over the years.[6,7] The employed chemistries, although very successful at overall 4*f*/5*f* group differentiation, each suffer from various limitations, which complicate process implementation. For instance, TALSPEAK,[8-10] Advanced TALSPEAK,[10-12] ALSEP,[13,14] and EXAm,[15-17] processes require careful pH control, necessitating the use of buffers. Those processes also suffer from slow kinetics, as do various renditions of the SANEX process,[18,19] which employ nitrogen heterocycle reagents. The management of waste streams is also problematic for TALSPEAK-type processes, as well as European options such as i-SANEX,[20-22] EXAm,[15-17] and EURO-GANEX[23,24] due to presence of non-CHON (carbon, hydrogen, oxygen, nitrogen) elements such as phosphorous and sulphur, which are not amenable to incineration.

[a] Japan Atomic Energy Agency, Nuclear Science and Engineering Center, 2-4 Shirakata, Tokai-mura, Naka-gun, Ibaraki 319-1195, Japan.
[b] Center for Radiation Chemistry Research, Idaho National Laboratory, 1955 N. Freemont Ave., Idaho Falls, 83415, USA.
[c] Department of Chemistry and Biochemistry, California State University Long Beach, 1250 Bellflower Boulevard, Long Beach California, 90840-9507, USA.
[d] Department of Chemistry, Brookhaven National Laboratory, Upton, New York, 11973, USA.
[e] University of Tokyo, Nuclear Professional School, School of Engineering, 2-22 Shirakata, Tokai-mura, Naka-gun, Ibaraki 319-1188, Japan.
* Corresponding authors: toigawa.tomohiro@jaea.go.jp and gregory.horne@inl.gov.
† Electronic Supplementary Information (ESI) available: HONTA degradation product mass spectra plots. See DOI: 10.1039/x0xx00000x

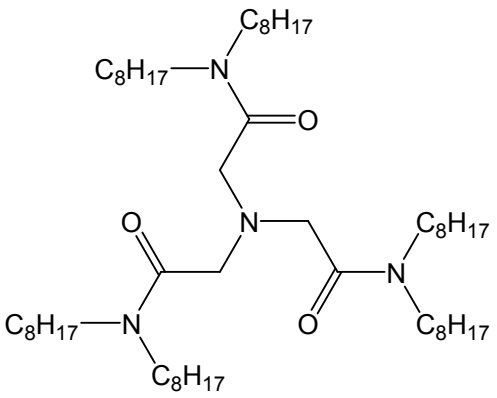

Fig. 1. Molecular structure of hexa-*n*-octylnitrilo-triacetamide (HONTA).

In light of these drawbacks, hexa-*n*-octylnitrilo-triacetamide (HONTA, Fig. 1) has been identified as a promising CHON candidate for achieving efficient MA/Ln separation under acidic conditions (pH < 1) without the need for additional complexants.[25-27] Further, the performance of HONTA has been successfully evaluated beyond bench-top studies, as part of the proposed *Solvent Extraction from Liquid waste using Extractants of CHON-type for Transmutation* (SELECT) process,[28] using continuous counter-current mixer-settler extractors.[27] However, despite the promise of HONTA resolving current limitations in efficient MA/Ln separations, the radiation robustness of this molecule and the efficacy of its radiolytic degradation products on process performance are unknown. This knowledge is essential as all UNF solvent extraction processes operate under highly radioactive conditions.

The intense, multi-component (predominantly alpha, beta, and gamma) radiation field experienced by a UNF solvent extraction system promotes radiolytic degradation of both the organic (R – diluent and ligand) and aqueous (H_2O/HNO_3) phases, yielding a suite of primary degradation products outlined by Equations 1-3:[29]

$$R \rightsquigarrow e^-, H^\bullet, R^{\bullet+}, R^\bullet \quad (1)$$

$$H_2O \rightsquigarrow e^-, H^\bullet, {}^\bullet OH, H_2O_2, H_2, H_{aq}^+ \quad (2)$$

$$HNO_3 \rightsquigarrow e^-, {}^\bullet NO_3, HNO_2, O^\bullet, H_{aq}^+. \quad (3)$$

Many of these species are highly reactive and capable of driving chemical change through the destruction of active solutes (complexants, phase modifiers, holdback agents, etc.) and the formation of subsequent degradation products, which negatively impact process performance over time.[30-33] One such impact is the perturbation of extraction and back-extraction properties, which in the case of HONTA may lead to a loss in MA/Ln separation efficiency. Consequently, the radiation-induced behaviour of HONTA solvent systems must be elucidated to further develop HONTA based MA/Ln separation technologies.

To this end, we present a systematic investigation into the effects of radiation on HONTA in solvent system formulations representative of envisioned large-scale process conditions (*n*-dodecane/HNO_3). A combination of steady-state solvent loop gamma irradiation, americium-241 and europium-154 distribution coefficient determination, and time-resolved pulsed electron radiolysis kinetic measurements were used to evaluate the radiation robustness of HONTA, subsequent impact on process performance, influence of *f*-element complexation, and fundamental radiation-induced processes.

Methodology

Caution! The americium-243 and europium-154 solutions used in this work were highly radioactive. Handling was performed in dedicated radiological and nuclear facilities using well established radiological safety protocols.

Chemicals. Americium-243 (^{243}Am, $\tau_{1/2}$ = 7370 years, E_α = 5.44 MeV) were sourced from on-hand oxide stocks at Idaho National Laboratory (INL). This material was purified by dissolution of $^{243}Am_2O_3$ powder in 6.0 M HNO_3 and then passed through a diglycolamide (DGA) extraction chromatographic resin column (Eichrom Technologies Inc., Lisle, IL, USA). Resin adsorbed ^{243}Am was desorbed with 20 mM hydrochloric acid (HCl). The HCl was then distilled off via a series of evaporative cycles (~85 °C) to yield a consolidated batch of americium trichloride ($^{243}AmCl_3$) – evaporated to near dryness – which was subsequently dissolved in 10 mM perchloric acid ($HClO_4$). This final ^{243}Am stock solution was standardized using a complexometric titration with diethylenetriaminepentaacetic acid (DTPA), where the $^7F_0' \rightarrow {}^5L_6'$ transition (λ_{max} = 503.05 nm for Am^{3+}, λ_{max} = 507.85 nm for $[^{243}Am(DTPA)]^{2-}$)[34,35] was monitored using a Cary 6000i UV-vis-NIR spectrophotmeter (Agilent, Santa Clara, CA, USA).

Europium-154 (^{154}Eu, $\tau_{1/2}$ = 8.6 years, E_β = 1.97 MeV) and americium-241 (^{241}Am, $\tau_{1/2}$ = 432.2 years, E_α = 5.64 MeV) were supplied by Eckert & Ziegler (Berlin, Germany). Hexa-*n*-octylnitrilo-triacetamide (HONTA, >96%) was synthesized as previously reported[36] and supplied by Chemicrea Inc (Tokyo, Japan). Diethylenetriaminepentaacetic acid (DTPA, *99%*) was purchased from Millipore-Sigma and recrystallized twice from hot water before preparation of complexometric solution. N,N,N',N'-tetraoctyldiglycolamide (TODGA, 99%) was supplied by Technocomm Ltd (Wellbrae, Scotland, UK). Dioctylamine (DOA, >97%) was supplied by Combi-Blocks (San Diego, CA, USA). Dioctylformamide (DOFA, >95%) and dioctylacetaminde (DOAA, >95%) were sourced from Angene Chemical (Telangana, India). Europium(III) pentahydrate (*99.9% trace metals basis*), nitric acid (HNO_3, *≥99.999% trace metals basis*), perchloric acid ($HClO_4$, *≥99.999% trace metals basis*), hydrochloric acid (HCl, *≥99.999% trace metals basis*), *n*-dodecane (*≥99% anhydrous*), dichloromethane (DCM, ≥99.8%), carbon tetrachloride (CCl_4, *≥99.5% anhydrous*), and potassium thiocyanate (KSCN, ≥99.0% *ACS Reagent Grade*) were obtained from MilliporeSigma (Burlington, MA, USA). FUJIFILM Wako Pure Chemical Cooperation (Osaka, Japan) supplied 2-propanol (≥99.7% HPLC grade). Unless otherwise stated, all chemicals were used without further purification. Compressed air, argon, and oxygen were purchased from Airgas (Radnor, PA, USA) with purities ≥ 99.5%. Ultra-pure water (18.2 MΩ cm) was used to prepare all aqueous solutions.

Steady-State Irradiations. The effects of ionizing radiation on the radiolytic integrity and performance of HONTA under envisioned process conditions were evaluated using the Idaho National Laboratory (INL) Center for Radiation Chemistry Research solvent test loop in conjunction with gamma rays delivered by a Nordion Gammacell 220E Cobalt-60 irradiator.[37] The sample solvent system comprised of 559 mL of 0.1 M HONTA/*n*-dodecane organic phase pre-equilibrated thrice with 0.1 M HNO_3, and 575 mL of fresh 0.1 M HNO_3 aqueous phase. The sample solvent system was irradiated for a series of doses up to ~350 kGy at a dose rate of ~2.03 kGy h^{-1} over 9 days. Dosimetry was determined by a combination of Fricke[38] and methyl red[39-42] methods corrected for changes in volume, volume ratio, and cobalt-60 decay (^{60}Co, $\tau_{1/2}$ = 5.27 years, $E_{\gamma 1}$ = 1.17 MeV and $E_{\gamma 2}$ =1.33 MeV). The presented absorbed doses are with respect to the organic phase and thus have been corrected for the electron density of *n*-dodecane (a factor of 0.78).[43] The rate of HONTA degradation is expressed as a dose constant (d) in kGy^{-1}.[44]

Time-Resolved Pulsed Electron Irradiations. Reaction kinetics for some of the primary radiolysis products of *n*-dodecane, HONTA, and TODGA were measured using a combination of picosecond and nanosecond pulsed electron radiolysis techniques available at Brookhaven National Laboratory (BNL) and the University of Tokyo, respectively.

Rate coefficients for the reaction of HONTA and its ^{243}Am and Eu complexes with the dodecane radical cation ($R^{\bullet+}$) were determined at ambient temperature using the picosecond pulsed electron radiolysis/transient absorption system at the BNL Laser Electron Accelerator Facility (LEAF).[45] Samples comprised of ~1 mL of HONTA/0.5 M DCM/*n*-dodecane solution in the presence and absence of ^{243}Am or Eu. For metal complex preparation, aqueous 1.0 mM ^{243}Am or Eu in 0.1 M HNO_3 were separately equilibrated in a 1:1 volume ratio with 30 mM HONTA/0.5 M DCM/*n*-dodecane solution that had been pre-equilibrated with 0.1 M HNO_3. Previous phase transfer kinetic measurements ensured quantitative extraction of metal ions was attained after 15 minutes of equilibration for an organic-to-aqueous phase volume ratio of unity.[27] The organic phases of each contact were recovered following agitation and centrifugation. The initial 30 mM HONTA/0.5 M DCM/*n*-dodecane stock solution and metal complex solutions were subsequently diluted by an appropriate amount of 0.5 M DCM/*n*-dodecane solution to attain a series of ligand and metal complex concentrations. All solutions were then transferred to screw-cap, semi-micro, 10 mm pathlength Suprasil cuvettes prior to irradiation. The residual ^{243}Am bearing aqueous phases were analysed by gamma spectroscopy, using a DSPEC-jr 2.0 digital gamma ray spectrometer equipped with an ORTEC GEM50P4 HPGe detector, to verify quantitative extraction of ^{243}Am by HONTA. Europium extraction efficiencies were determined by measuring Eu concentrations for both the aqueous and organic phases using an Agilent 7500ce ICP-MS system in the Institute for Integrated Research in Materials, Environments and Society (IIRMES) facility at California State University Long Beach, following EPA Method 200.8. Samples were diluted to obtain Eu concentrations in the range 1-500 ppb, with rhodium used as an internal standard. Calibration curves were run at the beginning and end of every sample series, using at least 6 points in this range.

Direct decay kinetics of $R^{\bullet+}$ following radiolysis with ~15 ps electron pulses at LEAF were followed at 800 nm over 200 ns using an FND-100Q silicon photodiode (EG&G) and LeCroy (Chestnut Ridge, NY, USA) WaveRunner 66Zi transient digitizer (600MHz, 12 bit resolution) to give an experiment time resolution of 1-2 ns. Interference filters (10 nm bandpass) were used for wavelength selection of the analysing light. Second-order reaction kinetics were extracted by fitting pseudo-first-order double-exponential fits to the decay traces, corrected for HONTA and HONTA metal complex ($[M(HONTA)_2]$) concentrations, and plotting as a function of solute concentration.

Formation and decay kinetics for the HONTA radical cation ($[HONTA]^{\bullet+}$) and HONTA triplet excited state ($[HONTA]^{\ddagger}$*) were measured using the nanosecond pulse radiolysis S-band linear accelerator at the University of Tokyo.[46] All measurements were performed using argon-saturated samples, comprising 2 mL of either neat HONTA or HONTA/*n*-dodecane mixtures, in 10 mm pathlength Suprasil cuvettes. Samples were irradiated with ~10 ns electron pulses, with kinetics followed over a broad spectral range (300-900 nm) using a Xe flash lamp (Nissin Electronics) in conjunction with a SPG-120S UV-Vis monochromator (Shimadzu, Kyoto, Japan), S1722-02 Silicon photodiode (Hamamatsu Photonics, Shizuoka, Japan) and DPO 7104 digital oscilloscope (Tektronix, Beaverton, OR, USA). Singular-value decomposition (SVD)[47] was applied to the resulting 3D time-dependent-absorption-spectrum to deconvolute signals of $[HONTA]^{\bullet+}$ and $^3[HONTA]$* using IgorPro software (Wavemetrics).

Confirmation of triplet excited state formation for HONTA and TODGA was achieved by performing a series of oxygen quenching experiments using the BNL LEAF. Dodecane solutions of both ligands were irradiated under either argon-saturated, aerated, or oxygen saturated conditions, with decay kinetics followed at 400 and 375 nm for HONTA and TODGA *n*-dodecane solutions, respectively.

Dosimetry for all pulsed electron experiments was determined using N_2O saturated solutions of 10 mM KSCN at λ_{max} = 472 nm ($G\varepsilon = 5.2 \times 10^{-4}$ m^2 J^{-1}).[48] Quoted errors for the reaction rate coefficients (*k*) are a combination of measurement precision and sample concentration errors.

High Performance Liquid Chromatography Electron Spray Ionization Tandem Mass Spectrometry (HPLC-ESI-MS/MS). The extent of HONTA radiolysis and complimentary degradation product formation in the organic phase was quantified by HPLC-ESI-MS/MS using a Shimadzu (Kyoto, Japan) LCMS 8040 triple quadrupole mass spectrometer at the Japanese Atomic Energy Agency (JAEA). The gamma irradiated HONTA/*n*-dodecane samples were diluted 1:10,000 using HPLC grade 2-propanol prior to HONTA quantification and diluted 1:1000 for degradation product (DOA, DOFA, and DOAA) analysis. Degradation product separation was achieved using a Kinetex reverse-phase C18 column (5.0 µm particle size, 150 mm × 2.1 mm id) held at 40 °C, and a mobile phase flow rate of 0.1 mL

min^{-1}. The mobile phase comprised an aqueous phase of 0.1 vol. % formic acid in water, and an organic phase of 0.1 vol. % formic acid in 2-propanol. Initial mobile phase conditions were 1:1 aqueous to organic. At injection, the ratio of the organic mobile phase was increased from 50% to 90% over 40 min, held at 90% for 14 min, and then decreased back to 50%. Presented error bars are standard deviations from triplicate HONTA and degradation product analyses. The signal intensity for HONTA exhibited a dependence on the concentration of HNO_3, with the measured signal intensity decreasing with increasing HNO_3 concentration (0, 0.1, and 3.0 M). However, for the conditions investigated by this work (0.1 M HNO_3) the signal intensity deviation from organic-only conditions was negligible.

Extraction and Back-extraction Distribution Ratios. To evaluate the impact of HONTA radiolysis on solvent system performance, extraction and back-extraction distribution ratios ($D_M = [M]_{org}/[M]_{aq}$) were determined for ^{241}Am and ^{154}Eu using the gamma irradiated HONTA/*n*-dodecane/0.1 M HNO_3 solvent system. The HONTA/*n*-dodecane organic phases were loaded by contacting aqueous phases containing 0.1 M HNO_3 and the ^{154}Eu and ^{241}Am radiotracers. The loaded HONTA/*n*-dodecane organic phases were then back-extracted by contacting aqueous phases containing 4.0 M HNO_3. Prior to metal loading the organic phases were pre-equilibrated by vigorous shaking for 5 min with an aqueous phase containing 0.1 M HNO_3 followed by 5 min of centrifugation. Equal volumes of organic phase and aqueous phase (containing metal ions) were then contacted by vigorous shaking for 5 min at room temperature (21.0 ± 1.0 °C) followed by 5 min of centrifugation. Back-extraction experiments to remove metal ions from the HONTA/*n*-dodecane organic phases were performed in the same manner using aqueous phases containing 4.0 M HNO_3. All solvent extraction experiments were carried out in triplicate, affording a precision of less than ±5%. After mixing, the two phases were separated, and a 1 mL sample of each phase was taken for radiometric counting to determine metal ion concentration. Gamma counting was performed, using an ORTEC GEM50P4 coaxial HPGe detector and DSPEC gamma spectrometer (AMETEK inc., Oak Ridge, TN, USA), to determine the ratio of radioisotope activity in each phase, allowing for calculation of ^{241}Am and ^{154}Eu distribution ratios.

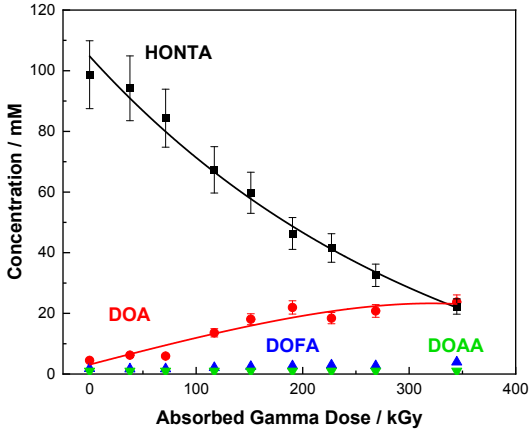

Fig. 2. Concentration of HONTA, DOA, DOFA, and DOAA as a function of absorbed gamma dose (~2.03 kGy h^{-1}) from the gamma radiolysis of formally 100 mM HONTA in *n*-dodecane contacted with a 0.1 M HNO_3 aqueous phase.

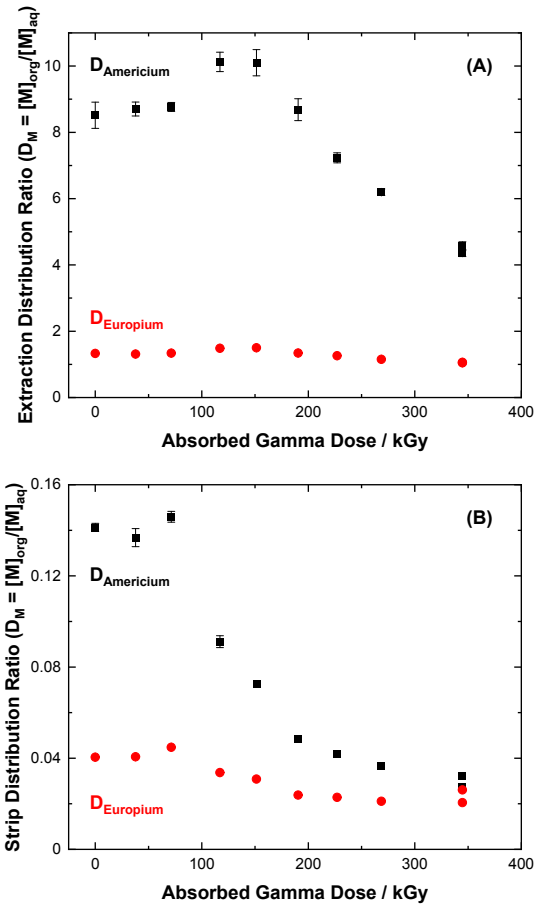

Fig. 3. Americium-241 and europium-154 distribution ratios for irradiated (~2.03 kGy h^{-1}), pre-equilibrated 100 mM HONTA/*n*-dodecane/0.1 M HNO_3 solution under extraction (**(A)**, 0.1 M HNO_3) and back-extraction (**(B)**, 4.0 M HNO_3) contact conditions.

Results and discussion

HONTA Degradation Rate and Products. The loss of HONTA and ingrowth of three quantifiable degradation products (dioctylamine (DOA), dioctylformamide (DOFA), and dioctylacetaminde (DOAA)) as a function of absorbed gamma dose in *n*-dodecane/0.1 M HNO_3 solution are shown in Fig. 2. HONTA exhibits a pseudo-first order decay with increasing absorbed dose, affording a dose coefficient of d = (4.48 ± 0.19) × 10^{-3} kGy^{-1}. This value is lower than dose coefficients previously reported for TODGA – another prime candidate for MA/Ln separations[49,50] – under a variety of solvent system conditions,[51] e.g., d = (5.4 ± 0.5) × 10^{-3} kGy^{-1} for gamma irradiated 50 mM TODGA in *n*-dodecane in contact with 3.0 M HNO_3.[52] This result bodes well for the continued development of HONTA in MA/Ln separation processes.

The radiolysis of HONTA results in the formation of 23 detectable degradation products in *n*-dodecane solutions –

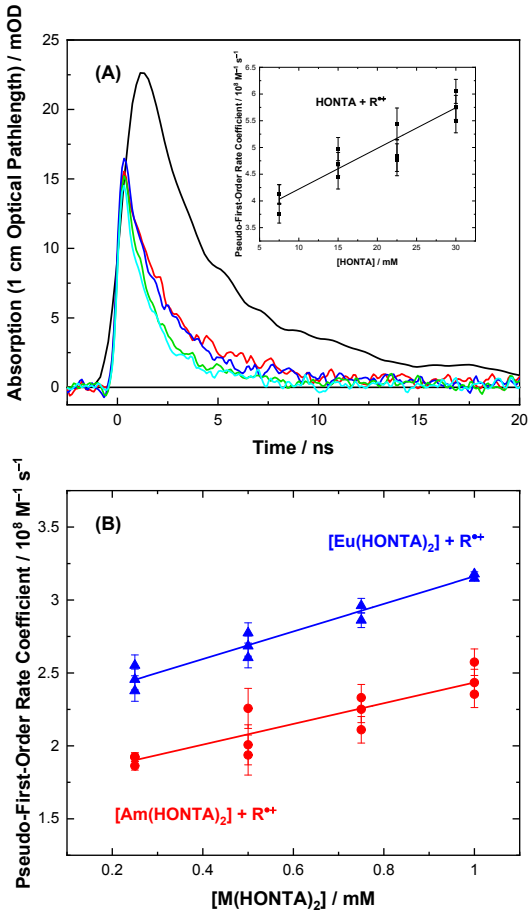

Fig. 4. (A) Decay traces for the *n*-dodecane radical cation ($R^{\bullet+}$) as a function of time and HONTA concentration in 0.5 M DCM/*n*-dodecane solution at 800 nm, top to bottom: 0, 7.5, 15, 22.5, and 30 mM HONTA. *Inset:* Second-order determination of the rate coefficient for the $R^{\bullet+}$ reaction with HONTA: k(HONTA + $R^{\bullet+}$) = (7.6 ± 0.8) × 10^9 M^{-1} s^{-1}. **(B)** Second-order determination of the rate coefficients for the $R^{\bullet+}$ reaction with ^{243}Am (●) and Eu (▲) HONTA complexes: k([^{243}Am(HONTA)$_2$] + $R^{\bullet+}$) = (7.1 ± 0.7) × 10^{10} M^{-1} s^{-1} and k([Eu(HONTA)$_2$] + $R^{\bullet+}$) = (9.45 ± 0.5) × 10^{10} M^{-1} s^{-1}. Solid lines in rate coefficient plots are weighted linear fits, with slopes corresponding to the second-order rate coefficient.

see Supplementary Information (SI) – all of which generally increased with increasing absorbed gamma dose. Of these species three were quantifiable (DOA – Fig. S2, DOFA – Fig. S4, and DOAA – Fig. S5), of which DOA was the predominant, accounting for a maximum of ~40% of HONTA degradation. As is evident from the exponential growth kinetics for DOA in Fig. 1, DOA is also progressively degraded with increasing absorbed dose. Consequently, mass balance could not be attained with the chemical standards (HONTA, DOA, DOFA, and DOAA) available. DOA was reported as a degradation product in TODGA radiolysis,[53] arising from cleavage of the C-N acyl bond.[54-56] Further, DOA has been previously shown to complex several important elements – uranium, molybdenum, and zirconium[57] – the controlled mass transport of which are critical for effective UNF reprocessing. Consequently, the radiolytic formation of DOA can be expected to interfere with complexation, thereby effecting the performance of a HONTA based reprocessing solvent system. Further, many of the unassigned degradation products could also possess complexing functionalities, and thus are also be expected to play a role in effecting the mass transfer of various metal ions.

Radiation Effects on Americium and Europium Extraction and Back-Extraction Properties. The impact of gamma irradiation on the performance of a HONTA/*n*-dodecane/0.1 M HNO_3 solvent system was evaluated by determining distribution ratios (D_M) for ^{241}Am and ^{154}Eu under extraction (0.1 M HNO_3) and back-extraction (4.0 M HNO_3) process conditions, given in Fig. 3 (A) and (B), respectively. For both metals there is an induction period of ~70 kGy before the onset of a progressive decrease in distribution ratios at higher absorbed gamma doses for both extraction and back-extraction conditions.

The induction period is attributed to a combination of the progressive loss of HONTA and ingrowth of DOA, as shown in Fig. 2, which equates to ~14 mM of each. Loss of HONTA reduces the system's ability to complex ^{241}Am and ^{154}Eu, while the radiolytic production of DOA facilitates the formation of different ^{241}Am and ^{154}Eu complexes that may exhibit enhanced/alternative extraction properties.

Dodecane Radical Cation Reaction Kinetics. The *n*-dodecane radical cation ($R^{\bullet+}$) is believed to be the major organic phase transient species responsible for inducing radiolytic degradation under *n*-dodecane (R) irradiation conditions, and has been shown to exhibit significant reactivity with UNF reprocessing ligands:[51,58-62]

Ligand + $R^{\bullet+}$ → [Ligand]$^{\bullet+}$ + R. (4)

The decay kinetics for this reaction with HONTA are shown in Fig. 4 (A), in which the lifetime of $R^{\bullet+}$ is seen to decrease sharply with increasing HONTA concentration, affording a second-order rate coefficient of k = (7.6 ± 0.8) × 10^9 M^{-1} s^{-1}. Although this value is lower than that reported for TODGA, k = (9.72 ± 1.1 × 10^9 M^{-1} s^{-1}),[51] it is nonetheless effectively diffusion limited[63] and expected to be a major degradation pathway for HONTA in *n*-dodecane solvent system formulations.

Interestingly, when HONTA is complexed to either ^{243}Am or ^{154}Eu its rate coefficient for reaction with $R^{\bullet+}$ increases by over an order of magnitude, k = (7.1 ± 0.7) × 10^{10} and (9.5 ± 0.5) × 10^{10} M^{-1} s^{-1}, respectively (Fig. 4 (B)). The effect of complexation on reaction kinetics indicates the availability of alternative/additional reaction pathways in comparison to the free ligand. The reaction of HONTA with $R^{\bullet+}$ most likely proceeds via an outer-sphere electron transfer process, Equation 4, whereby an electron is transferred from HONTA to $R^{\bullet+}$, generating the corresponding HONTA radical cation ([HONTA]$^{\bullet+}$). However, the *f*-element complexes of HONTA may also undergo inner-sphere electron transfer processes, whereby electron transfer to or from [HONTA]$^{\bullet+}$ and the metal cation centre may subsequently occur and regenerate HONTA or promote its fragmentation.[64] Complexation also involves a redistribution of electron bond density and changes in ligand geometry, which can weaken chemical bonds and alter steric hindrance, ultimately effecting chemical reactivity. Further, the *f*-element complexes of HONTA are expected to be significantly larger than the free ligand. Based on a 2:1 ligand-to-metal ratio

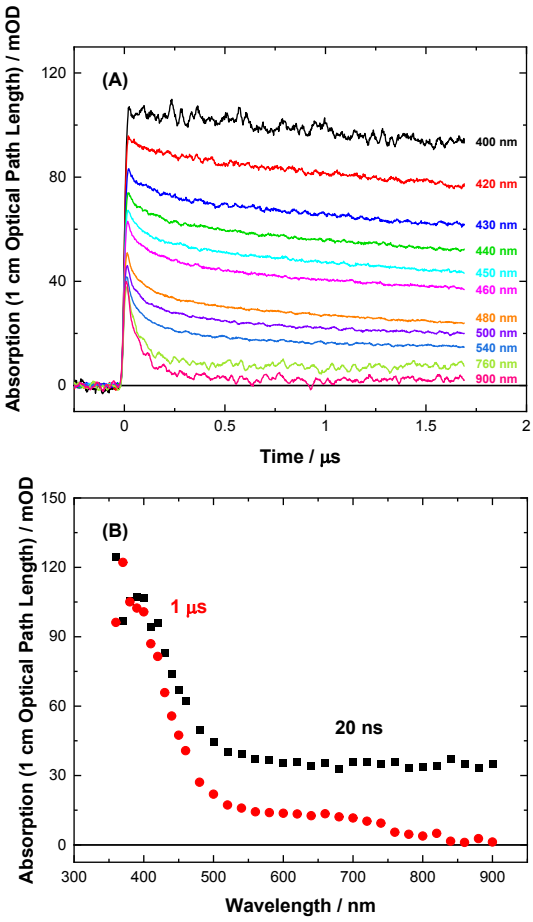

Fig. 5. **(A)** Selected wavelengths monitored during the radiolysis of pure HONTA as a function of time, and **(B)** the corresponding spectral absorptions at 20 ns (■) and 1 us (●).

for the HONTA complex under the conditions employed by these time-resolved studies,[65] the metal complex might be expected to be ~2-3 times larger than the free ligand itself. As these reactions are effectively diffusion-controlled, based on the Smoluchowski diffusion equation, this would predict a similar increase in the reaction rate coefficient, which is much smaller than the order-of-magnitude increase seen experimentally, further highlighting the existence of additional processes.

Overall, the measured increase in rate coefficients for the reaction of HONTA with $R^{\bullet+}$ upon *f*-element complexation raises the question as to whether this would translate into an increased rate of steady-state HONTA degradation. Furthermore, does metal ion complexation afford an alternative distribution of HONTA degradation products? To address these questions, analogous experiments specifically investigating the steady-state radiation-induced behaviour of metal-loaded HONTA solvent systems are presently underway.

Primary Products of HONTA Radiolysis. The $[HONTA]^{\bullet+}$ is the initial product after reaction with the $R^{\bullet+}$ (Equation 4) and can also be formed as one of the possible primary products from the direct ionization of HONTA:

$$HONTA \rightsquigarrow e^-, [HONTA]^{\bullet+}, [HONTA]^* \quad (5)$$

Consequently, the fate of this transient is directly related to the formation of HONTA degradation products, such as DOA, and thus the observed effects of radiation on the ^{241}Am and ^{154}Eu distribution ratios, and ultimately process performance. Consequently, understanding the kinetic behaviour of this species is also critical for evaluating the feasibility of a HONTA based reprocessing solvent system. The time-dependent absorption spectra and corresponding spectral absorptions at 20 ns and 1 us for nanosecond pulsed electron irradiation of pure HONTA are shown in Fig. 5, from which more than one distinct radiolytic species can be seen to be formed. Deconvolution of these spectra by SVD analysis yielded two HONTA transients – a short-lived (nanoseconds) and a long-lived (microseconds) species as shown in Fig. 6. Similar time profiles were reported by Sugo *et al.* for TODGA,[66] although these were assigned to the TODGA radical cation ($[TODGA]^{\bullet+}$). Here we assign the short-lived species (i = 1) to the $[HONTA]^{\bullet+}$, seen to rapidly decay within 100 ns, and the second longer-lived species (i = 0) to the HONTA triplet excited state ($^3[HONTA]^*$), owing to its relatively long lifetime compared with typical singlet excited states.[67] Complimentary experiments were also performed for HONTA/*n*-dodecane solutions, and showed the formation of the same two transients. These findings confirm their formation by both direct and indirect radiolytic processes, which is consistent with our picosecond pulse radiolysis results for the reaction of $R^{\bullet+}$ with HONTA.

The long-lived species (i = 0) in Fig. 6 is thought to be the $^3[HONTA]^*$ formed by direct excitation (Equation 5) and recombination processes (Equation 6):[67]

$$[HONTA]^{\bullet+} + e^- \rightarrow [HONTA]^* \rightarrow {}^3[HONTA]^*. \quad (6)$$

This assignment is contrary to that previously reported for TODGA.[66] Verification of our assignment was achieved by performing a series of oxygen (O_2) quenching pulsed electron experiments for both HONTA and TODGA, shown in Fig. 7. (A) and (B), respectively. For both HONTA and TODGA irradiations, the lifetime of the longer-lived species (i = 0) decreases with increasing dissolved O_2 concentration, which we attribute to quenching of the respective triplet states:

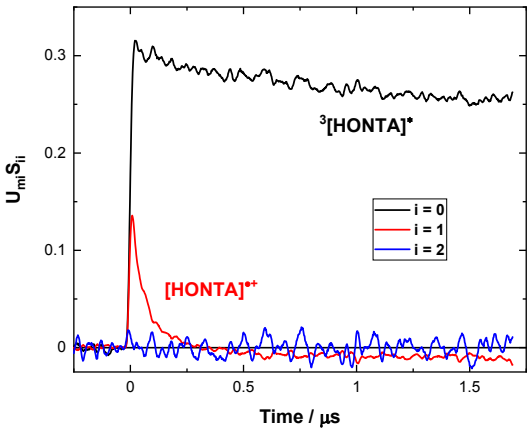

Fig. 6. SVD analysis solution of the 3D time-dependent-absorption-spectrum derived from **Fig. 5 (A)**, assigned i = 0 to $^3[HONTA]^*$ and i = 1 to $[HONTA]^{\bullet+}$.

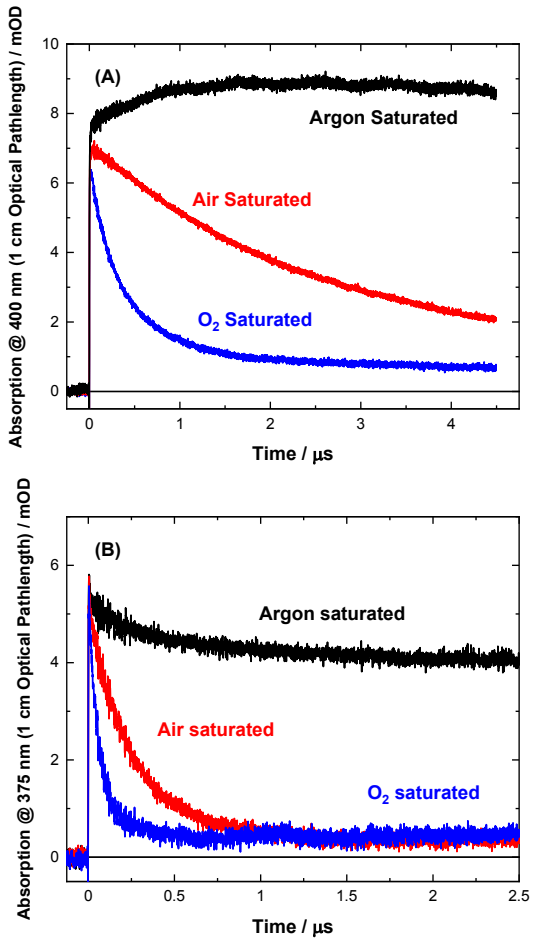

Fig. 7. Kinetics for O_2-induced quenching in 30 mM HONTA/0.5 M DCM/*n*-dodecane at 400 nm **(A)** and 30 mM TODGA/0.5 M DCM/*n*-dodecane at 375 nm **(B)** as a function of time and dissolved oxygen composition (argon saturated, air saturated, and oxygen saturated).

$$^3[\text{HONTA/TODGA}]^* + O_2 \rightarrow \text{HONTA/TODGA} + O_2^*. \quad (7)$$

Assuming dissolved O_2 concentrations of 0, 2, and 10 mM in *n*-dodecane under Ar, air, and O_2 saturated conditions, respectively, the following second order rate coefficients were derived: $k(^3[\text{HONTA}]^* + O_2) = 2.2 \times 10^8\ M^{-1}\ s^{-1}$ and $k(^3[\text{TODGA}]^* + O_2) = 1.6 \times 10^9\ M^{-1}\ s^{-1}$. Triplet quenching, as opposed to carbon centred radical (R•) capping (Equation 8), is supported by the magnitude of our O_2 rate coefficients, which are lower than those typically reported for O_2 addition to carbon-centered radicals in water (2-4 $\times$ $10^9\ M^{-1}\ s^{-1}$):[68]

$$R^\bullet + O_2 \rightarrow RO_2^\bullet. \quad (8)$$

Interestingly, the quenching rate coefficient for $^3[\text{HONTA}]^*$ is an order of magnitude slower than that for $^3[\text{TODGA}]^*$. Further, we do not see a complimentary growth of the triplet signal for TODGA under Ar-saturated conditions. This difference may be attributed to the relative energetics of the corresponding radical cations, where reaction of this species with chloride anions (Cl^-) formed by CH_2Cl_2 scavenging of electrons is attributed to said growth:[69]

$$CH_2Cl_2 + e_{aq}^- \rightarrow {}^\bullet CH_2Cl + Cl^- \quad (9)$$

$$[\text{HONTA}]^{\bullet+} + Cl^- \rightarrow {}^3[\text{HONTA}]^* + Cl^\bullet. \quad (10)$$

Our data suggests that the $[\text{HONTA}]^{\bullet+}$ readily undergoes this process, while the $[\text{TODGA}]^{\bullet+}$ does not. This may be a consequence of the $[\text{TODGA}]^{\bullet+}$ undergoing more rapid and/or alternative decay processes, e.g., proton transfer and/or dimerization. As such, follow up experiments are underway to resolve the differences in reactivity between these two transient species.

Conclusions

Gamma irradiation of HONTA/*n*-dodecane/0.1 M HNO_3 solutions caused pseudo first-order degradation of the ligand and generation of several products, of which dioctylamine was found to be the dominant quantifiable species. The combined loss of HONTA and ingrowth of dioctylamine resulted in progressively lower distribution ratios for americium and europium under both extraction (0.1 M HNO_3) and back-extraction (4.0 M HNO_3) solvent system conditions after an induction period of ~70 kGy.

HONTA radiolysis was believed to be predominantly driven by reaction with the *n*-dodecane radical cation, the rate coefficient for which was determined as $k = (7.6 \pm 0.8) \times 10^9\ M^{-1}\ s^{-1}$, for the free ligand, and $k = (7.1 \pm 0.7)$ and $(9.5 \pm 0.5) \times 10^{10}\ M^{-1}\ s^{-1}$ for the corresponding americium-243 and europium HONTA complexes, respectively. The enhanced metal ion HONTA complex rate coefficients are indicative of additional reaction pathways facilitated by a combination of inner- vs. outer-sphere processes, redistribution of electron bond density, and changes in steric arrangements.

Finally, the primary species generated by the direct radiolysis of HONTA were assigned to the short-lived (<100 ns) HONTA radical cation and longer-lived (microseconds) HONTA triplet excited state. Both species were also observed in HONTA/*n*-dodecane solutions, and consequently expected to contribute to the suite of measured HONTA degradation products. Excited state assignment was supported by time-resolved oxygen-quenching experiments.

Conflicts of interest

There are no conflicts to declare.

Acknowledgements

This research has been funded by the US-DOE Assistant Secretary for NE, under the Material Recovery and Waste Form Development Campaign, DOE-Idaho Operations Office Contract DE-AC07-05ID14517 and DE-NE0008659 Nuclear Energy Universities Program (NEUP) grant.

Picosecond pulsed electron irradiations reported herein were performed using the BNL LEAF of the BNL Accelerator Center for Energy Research, supported by the US-DOE Office of Basic Energy Sciences, Division of Chemical Sciences, Geosciences, and Biosciences under contract DE-SC0012704.

Nanosecond pulsed electron irradiations were performed using the Electron Linac Facility at the University of Tokyo, supported by a collaborative research project between the Nuclear Professional School, School of Engineering, and the University of Tokyo.

The authors would like to thank the DOE-JAEA collaboration for supporting this research effort. We would also like to acknowledge Alex Long of CSULB IIRMES for performing the Eu and ICP-MS measurements.

Notes and references

(1) G.T. Seaborg, *Radiochim. Acta*, 1993, **61 (3-4)**, 115.

(2) S. Cotton, 2004. Comprehensive Coordination Chemistry II, McCleverty, J.A., Meyer, T.J. (Ed.) Elsevier, Oxford, vol. 3, pp. 93–188.

(3) C.J. Burns, M.P. Neu, H. Boukhalfa, K.E. Gutowski, NJ. Bridges, R.D. Rogers, 2004. Comprehensive Coordination Chemistry II, McCleverty, J.A., Meyer, T.J. (Ed.), Elsevier, Oxford, vol. 3, pp. 189–332.

(4) J.J. Katz, L.R. Morss, N.M. Edelstein, J. Fuger, 2006. The Chemistry of the Actinide and Transactinide Elements, Katz, J.J., Morss, L.R., Edelstein, N.M., Fuger, J. (Ed.), Springer, Dordrecht, vol. 1, pp. 1–17.

(5) International Atomic Energy Agency, Technical Reports Series No. 435; Implications of Partitioning and Transmutation in Radioactive Waste Management, IAEA, Vienna, 2004. https://www.iaea.org/publications/7112/implications-of-partitioning-and-transmutation-in-radioactive-waste-management.

(6) A. Geist, J.-M. Adnet, S. Bourg, C. Ekberg, H. Galan, P. Guilbaud, M. Miguirditchian, G. Modolo, C. Rhodes, R. Taylor, *Sep. Sci. Technol.*, 2020, DOI: 10.1080/01496395.2020.1795680.

(7) A. Bhattacharyya, P. K. Mohapatra, *Radiochim. Acta*, 2019, **107 (9-11)**, 931.

(8) B. Weaver, F.A. Kappelmann, 1964. TALSPEAK: A New Method of Separating Americium and Curium from the Lanthanides by Extraction from am Aqueous Solution of an Aminopolyacetic Acid Complex with a Monoacidic Organophosphate or Phosphonate. ORNL-3559, Oak Ridge National Laboratory, USA.

(9) K.L. Nash, *Solv. Extr. Ion Exch.*, 2015, **33 (1)**, 1.

(10) B. Moyer, G. Lumetta, B. Mincher, B., 2015. Minor Actinide Separation in the Reprocessing of Spent Nuclear Fuels: Recent Advances in the United States. Reprocessing and Recycling of Spent Nuclear Fuel; Taylor, R., Ed.; Woodhead Publishing: Oxford, UK, pp 289–312.

(11) G.J. Lumetta, T.G. Levitskaia, A. Wilden, A.J. Casella, G.B. Hall, L. Lin, S.I. Sinkov, J.D. Law, G. Modolo, *Solv. Extr. Ion Exch.*, 2017, **35 (6)**, 377.

(12) A. Wilden, G. Lumetta, F. Sadowski, H. Schmidt, D. Schneider, M. Gerdes, J. Law, A. Geist, D. Bosbach, G. Modolo, *Solv. Extr. Ion Exch.*, 2017, **35**, 396.

(13) G. J. Lumetta, A. V. Gelis, J. C. Carter, C. M. Niver, M. R. Smoot, *Solvent Extr. Ion Exch.*, 2014, **32**, 333.

(14) A. V. Gelis, G. J. Lumetta, *Ind. Eng. Chem. Res.*, 2014, **53**, 1624.

(15) M.-J. Bollesteros, J.-N. Calor, S. Costenoble, M. Montuir, V. Pacary, C. Sorel, F. Burdet, D. Espinoux, X. Hérès, C. Eysseric, *Proc. Chem.*, 2012, **7**, 178.

(16) S. Chapron, C. Marie, G. Arrachart, M. Miguirditchian, S. Pellet-Rostaing, *Solvent Extr. Ion Exch.*, 2015, **33(3)**, 236.

(17) M. Miguirditchian, V. Vanel, C. Marie, V. Pacary, M.-C. Charbonnel, L. Berthon, X. Hérès, M. Montuir, C. Sorel, M.-J. Bollesteros, *Solvent Extr. Ion Exch.*, 2020, **38**, 365.

(18) A. Wilden, C. Schreinemachers, M. Sypula, G. Modolo, *Solvent Extr. Ion Exch.*, 2011, **29 (2)**, 190.

(19) S. Lange, A. Wilden, G. Modolo, F. Sadowski, M. Gerdes, D. Bosbach, *Solvent Extr. Ion Exch.*, 2017, **35 (3)**, 161.

(20) A. Wilden, G. Modolo, M. Sypula, A. Geist, D. Magnusson, *Procedia Chem.*, 2012, **7**, 418.

(21) D. Magnusson, A. Geist, R. Malmbeck, G. Modolo, A. Wilden, *Procedia Chem.*, 2012, **7**, 245.

(22) A. Wilden, G. Modolo, P. Kaufholz, F. Sadowski, S. Lange, M. Sypula, D. Magnusson, U. Mullich, A. Geist, D. Bosbach, *Solv. Extr. Ion Exch.*, 2015, **33**, 91.

(23) M. Carrott, K. Bell, J. Brown, A. Geist, C. Gregson, X. Hères, C. Maher, R. Malmbeck, C. Mason, G. Modolo, U. Müllich, M. Sarsfield, A. Wilden, R. Taylor, *Solv. Extr. Ion Exch.*, 2015, **32 (5)**, 447.

(24) R. Taylor, M. Carrott, H. Galan, A. Geistc, X. Hères, C. Maher, C. Mason, R. Malmbeck, M. Miguirditchian, G. Modolo, C. Rhodes, M. Sarsfield, A. Wilden, *Procedia Chem.*, 2016, **21**, 524.

(25) Y. Sasaki, Y. Tsubata, Y. Kitatsuji, Y. Morita, *Chem. Lett.*, 2013, **42 (1)**, 91.

(26) Y. Sasaki, Y. Tsubata, Y. Kitatsuji, Y. Sugo, N. Shirasu, Y. Morita, *Solv. Extr. Ion Exch.*, 2014, **32**, 179.

(27) Y. Ban, H. Suzuki, S., Hotoku, N., Tsutsui, Y. Tsubata, T. Matsumura, *Solv. Extr. Ion Exch.*, 2019, **37 (7)**, 489.
(28) Y. Ban, H. Suzuki, S. Hotoku, T. Kawasaki, H. Sagawa, N. Tsutsui, T. Matsumura, *Solv. Extr. Ion Exch.*, 2019, **37**, 27.
(29) B.J. Mincher, S.P. Mezyk, *Radiochim. Acta*, 2009, **97 (9)**, 519.
(30) B.J. Mincher, G. Modolo, S.P. Mezyk, *Solv. Extr. Ion Exch.*, 2009, **27 (1)**, 1.
(31) B.J. Mincher, G. Modolo, S.P. Mezyk, *Solv. Extr. Ion Exch.*, 2009, **27 (3)**, 331.
(32) B.J. Mincher, G. Modolo, S.P. Mezyk, *Solv. Extr. Ion Exch.*, 2009, **27 (5-6)**, 579.
(33) B.J. Mincher, G. Modolo, S.P. Mezyk, *Solv. Extr. Ion Exch.*, 2010, **28 (4)**, 415.
(34) G. Tian, D.K. Shuh, *Dalton Trans.*, 2014, **43**, 14565.
(35) P.R. Zalupski, T.S. Grimes, C.R. Heathman, D.R. Peterman, *Appl. Spectrosc.*, 2017, **71 (12)**, 2608.
(36) M. Iqbal, J. Huskens, W. Verboom, M. Sypula, G. Modolo, *Supramol. Chem.*, 2010, **22**, 827.
(37) D. Peterman, A. Geist, B. Mincher, G. Modolo, M.H. Galan, L. Olson, R. McDowell, *Ind. Eng. Chem. Res.*, 2016 **55**, 10427.
(38) H. Fricke, E.J. Hart, H.P. Smith, *J. Chem. Phys.*, 1938, **6 (5)**, 229.
(39) M.F. Barakata, K. El-Salamawya, M. El-Bannaa, M. Abdel-Hamida, A. Abdel-Rehim Tahab, *Rad. Phys. Chem.*, 2001, **61 (2)**, 129.
(40) Z. Ajji, *Rad. Measurements*, 2006, **41 (4)**, 438.
(41) W. Chairunisa, C. Imawan, *J. Phys. Conf. Series*, 2019, **1321 (2)**, 1.
(42) J. Pearson, O. Jan, G.E. Miller, M. Nilsson, *J. Radioanal. Nucl. Chem.*, 2012, **292**, 719.
(43) J.W.T. Spinks, R.J. Woods, 1990. An Introduction to Radiation Chemistry; Third Edition; Wiley-Interscience: New York.
(44) R.D. Curry, B.J. Mincher, *Appl. Rad. Iso.*, 2000, **52 (2)**, 189.
(45) J.F. Wishart, A.R. Cook, J.R. Miller, *Rev. Sci. Instr.*, 2004, **75 (11)**, 4359.
(46) K. Hata, M. Lin, Y. Katsumura, Y. Muroya, H. Fu, S. Yamashita, H. Nakagawa, *J. Rad. Res.*, 2011, **52 (1)**, 15.
(47) J.F. Wishart, A.M. Funston, T. Szreder, A.R. Cook, M. Gohdoa, *Faraday Discuss.*, 2012, **154**, 353.
(48) G.V. Buxton, C.R. Stuart, *J. Chem. Soc. Faraday Trans.*, 1995, **92 (2)**, 279.
(49) Y. Sasaki, Y. Sugo, S. Suzuki, S. Tachimori, *Solv. Extr. Ion Exch.*, 2001, **19 (1)**, 91.
(50) G. Modolo, H. Asp, C. Schreinemachers, H. Vijgen, *Solv. Extr. Ion Exch.*, **2007**, *25 (6)*, 703.
(51) C.A. Zarzana, G.S. Groenewold, B.J. Mincher, S.P. Mezyk, A. Wilden, H. Schmidt, G. Modolo, J.F. Wishart, A.R. Cook, *Solv. Extr. Ion Exch.*, 2015, **33**, 431.
(52) G.P. Horne, C.A. Zarzana, C. Rae, A.R. Cook, S.P. Mezyk, P.R. Zalupski, A. Wilden, B.J. Mincher, *Phys. Chem. Chem. Phys.*, 2020, DOI: 10.1039/D0CP04310A.
(53) Y. Sugo, Y. Sasaki, S. Tachimori, *Radiochimica Acta*, 2002, **90 (3)**, 161.
(54) C. Madic, M.J. Hudson, *European Commission, Nuclear Science and Technology*. EUR 18038 EN.
(55) Musikas, C., 1988. Potentiality of nonorganophosphorus extractants in chemical separations of actinides. *Sep. Sci. Technol.*, 1998, **23(12&13)**, 1211.
(56) G. Thiollet, C. Musikas, *Solv. Extr. Ion Exch.*, 1989, **7(5)**, 813.
(57) A.M. Al-Ani, F.M. Masoud, *Hydrometallurgy*, 1982, **9 (20)**, 211.
(58) S.P. Mezyk, B.J. Mincher, S.B. Dhiman, B. Layne, J.F. Wishart, *J. Radioanal. Nucl. Chem.*, 2016, **307 (3)**, 2445.
(59) S.P. Mezyk, G.P. Horne, B.J. Mincher, P.R. Zalupski, A.R. Cook, J.F. Wishart, *Procedia Chem.*, 2016, **21**, 61.
(60) J. Drader, G. Saint-Louis, J.M. Muller, M.-C. Charbonnel, P. Guilbaud, L. Berthon, K.M. Roscioli-Johnson, C.A. Zarzana, C. Rae, G.S. Groenewold, B.J. Mincher, S.P. Mezyk, K. McCann, S.G. Boyes, J. Braley, *Solv. Extr. Ion Exch.*, 2017, **35(7)**, 480.
(61) G.P. Horne, C.A. Zarzana, T.S. Grimes, C. Rae, J. Ceder, S.P. Mezyk, B.J. Mincher, M.-C. Charbonnel, P. Guilbaud, G. Saint-Louis, L. Berthon, L., *Dalton Trans.*, 2019, **48**, 14450.
(62) G.P. Horne, A. Wilden, S.P. Mezyk, L. Twight, M. Hupert, A. Stärk, W. Verboom, B.J. Mincher, G. Modolo, *Dalton Trans.*, 2019, **48**, 17005.
(63) T. Kondoh, J. Yang, K. Norizawa, K. Kan, Y. Yoshida, *Rad. Phys. Chem.*, 2011, **80 (2)**, 286.
(64) G.V. Buxton, Q.G. Mulazzani, 1999. Free Radicals as a Source of Uncommon Oxidation States of Transition Metals. Metal Ions in Biological Systems, Volume 36: Interrelations Between Free Radicals and Metal Ions in Life Processes 1st Edition. Sigel, A. (Ed.), Routledge, New

York, pages 103–123.

(65) A. Bhattacharyya, R.J.M. Egberink, P.K. Mohapatra, P.K. Verma, A.K. Yadav, S. Jha, D. Bhattacharyya, J. Huskens, W. Verboom, *Dalton Trans.*, 2017, **46**, 16631.

(66) Y. Sugo, Y. Izumi, Y. Yoshida, S. Nishijima, Y. Sasaki, T. Kimura, T. Sekine, H. Kudo, *Rad. Phys. Chem.*, 2007, **76 (5)**, 794.

(67) S.L. Murov, I. Carmichael, G.L. Hug, 1993. Handbook of Photochemistry Second Edition, Revised and Expanded. Marcel Dekker, Inc., New York.

(68) C. von Sonntag, P. Dowideit, X. Fang, R. Mertens, X. Pan, M.N. Schuchmann, H.-P. Schuchmann, *Water Sci. Tech.*, 1997, **35 (4)**, 9.

(69) M.J. Bird, A.R. Cook, M. Zamadar, S. Asaoka, J.R. Miller, *Phys. Chem. Chem. Phys.*, 2020, **26**, 14660.

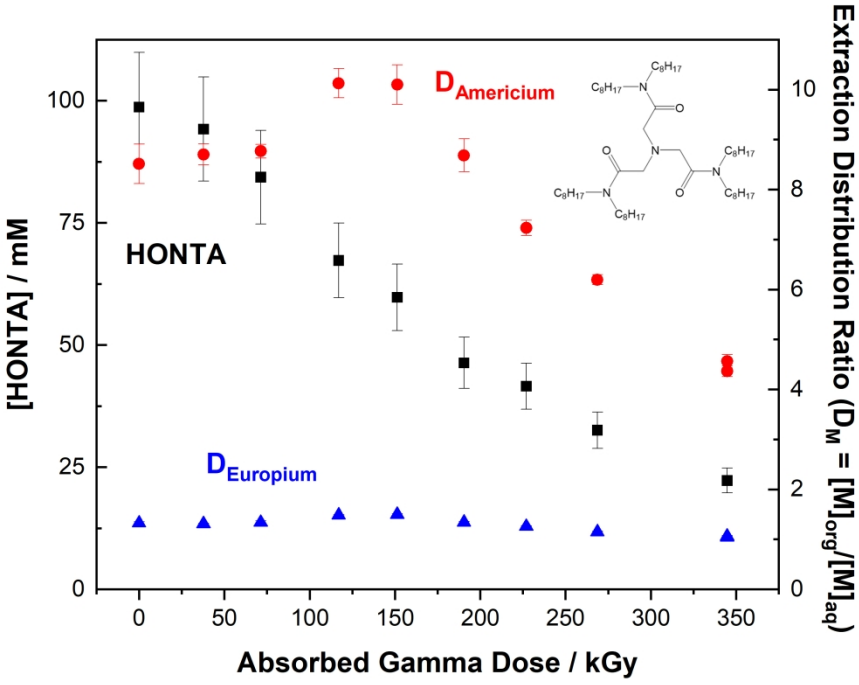

272x208mm (300 x 300 DPI)